

E. Del Core, M. Bertucci, A. Bosotti, A. T. Grimaldi, L. Monaco, C. Pagani, R. Paparella, D. Sertore, INFN Milano LASA, 20090 Segrate, Italy

Field emission (FE) is a key limiting phenomenon in SRF cavities. An algorithm exploiting a self-consistent model of cavity FE has been developed. This method exploits **experimental observables** (such as *Q-value*, *X-ray endpoint*, and *dose rate*) to reconstruct **emitter position** and **size** as well as the **field enhancement factor**. To demonstrate the model self-consistency, the algorithm has been applied to the test results of a **PIP-II LB650** prototype cavity. The results of the procedure are here described.

Introduction

One of the most limiting factor to the accelerating gradient in **superconducting radio-frequency (SRF)** cavity is **Field Emission (FE)**.

- This phenomenon is associated with the surface electric field \vec{E} and refers to the **emission of electrons** from regions of **high electric field** on the cavity surface.
- These emitted electrons, originating from the **emitters** site, are accelerated by the RF field until they impact the cavity surface.
- As a result of this impact, **X-ray** radiation can be generated.
- The **power** deposited by the impacting electron depends both on the **trajectory** of the particle and on the **intrinsic properties** of the emitter.

In SRF cavities, FE scales exponentially with the \vec{E} and contributes to the consume of RF power. So, it may correspond to an undesirable **degradation** of the **Q-value**, leading to an increase in **cryogenic consumption**.

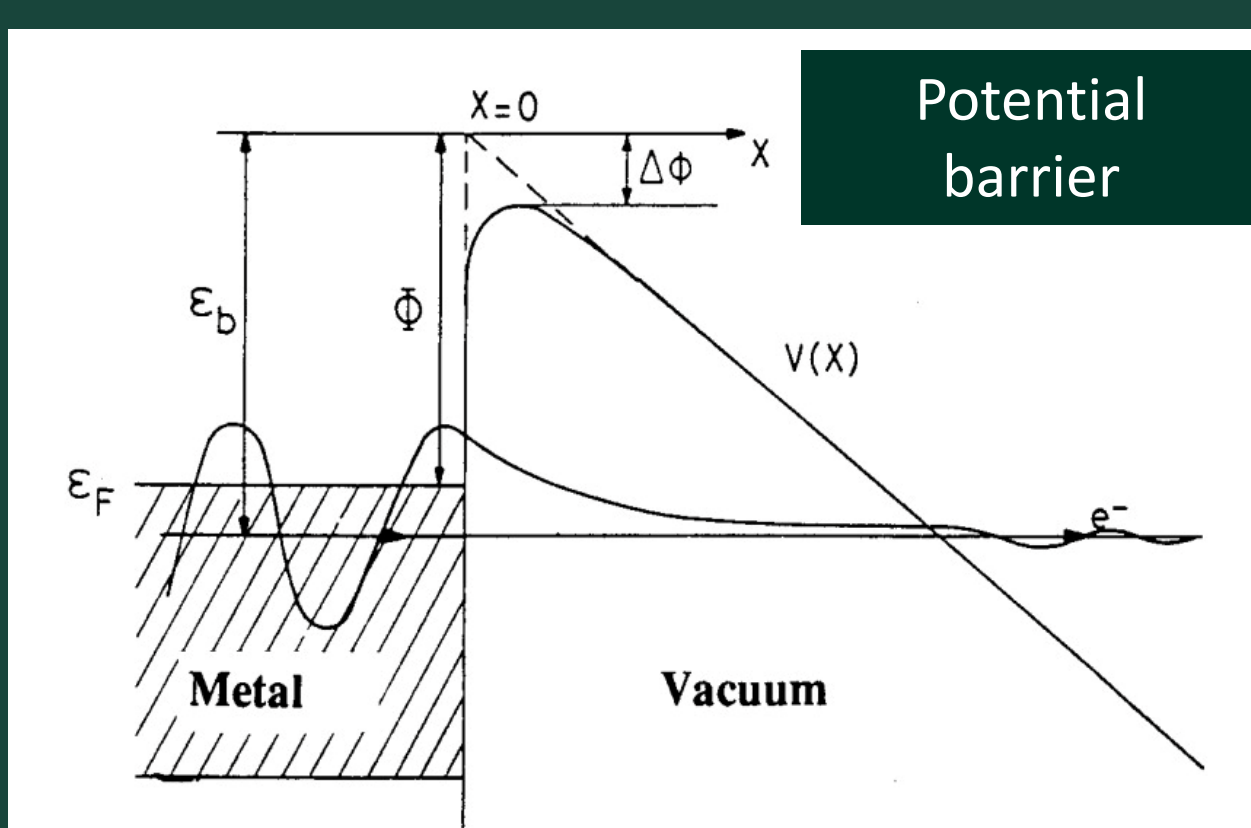
In a metal, electrons are typically confined by a potential barrier that cannot be escaped in normal conditions. This gap between the **Fermi level** in the metal and the **vacuum level** (a.k.a. **work function**) can be overcome when electrons acquire energy.

Under the influence of external \vec{E} , the potential barrier assumes a triangular shape and its width diminishes.

When sufficiently **thin**, there is a **non negligible probability** for electrons to **tunnel** it and **escape**.

Fowler-Nordheim (FN) equation describes the current

$$I = S \frac{A_{FN} E^2 \beta^2}{\phi} e^{-\frac{B_{FN} \phi^{3/2}}{\beta E}}$$



$A_{FN} = 1.54 \times 10^6$, $B_{FN} = 6.83 \times 10^3$, β field enhancement factor, ϕ work function and $E_s(t) = E_{s0} \sin 2\pi f t$ electric field

How to evaluate the REAL FE impact

- External detectors have a **limited field of view** → only a restricted portion of the emission pattern can be observed.
 - The emitted radiation undergoes several **attenuation** phenomena before reaching the detector active volume.
 - If the electron impact energies are **too low**: **FE may not** be detected
- Challenge:** determine the activated emitter positions "a priori"
- Inner detectors can assist in **reconstructing** the emission pattern; FE can be **coupled** with other phenomena → *multipacting (MP)*, *parasitic mode excitation*, *thermal-induced quench* → more **complex** to comprehensively model the cavity behavior.

Solver steps

Objective: obtain the distribution probability of the emission event

For each value of the **accelerating field**:

- Multiple **emitter sites tested** along the cavity profile
- Electron current** modeled according to the FN emission law
- Colliding electron **trajectories collected** within a specific region on the cavity surface. For each of them, the **impact energy** $E(\varphi_i)$ and the **number** of emitted particles $N(\varphi_i)$ are evaluated.
- Post-processing of simulated data to obtain the **overall impact electron energy spectrum**.

→ **1st cross-check** with experimental data: *X-ray energy spectrum*

- Compute the power drained by electron dark current P_{FE} by summing up over the cavity surface → **Q_0 vs E_{acc} trend**

$$P_{FE} = \frac{1}{T_{RF}} \sum_i N(\varphi_i) E(\varphi_i)$$

Case study PIP-II EZ-002 CAVITY

To validate the model, the prototype multicell **B61-EZ-002 PIP-II** was used.

- 1st test:** some MP with radiation, then sudden rise of radiation at 20.8 MV/m
- Test repeated from low fields
- 2nd test:** same behavior as 1st test up to until 14 MV/m... then sudden rise of radiation and Q_0 drop. Cavity quench at 23 MV/m with FE → **irreversible activation of a field emitter**

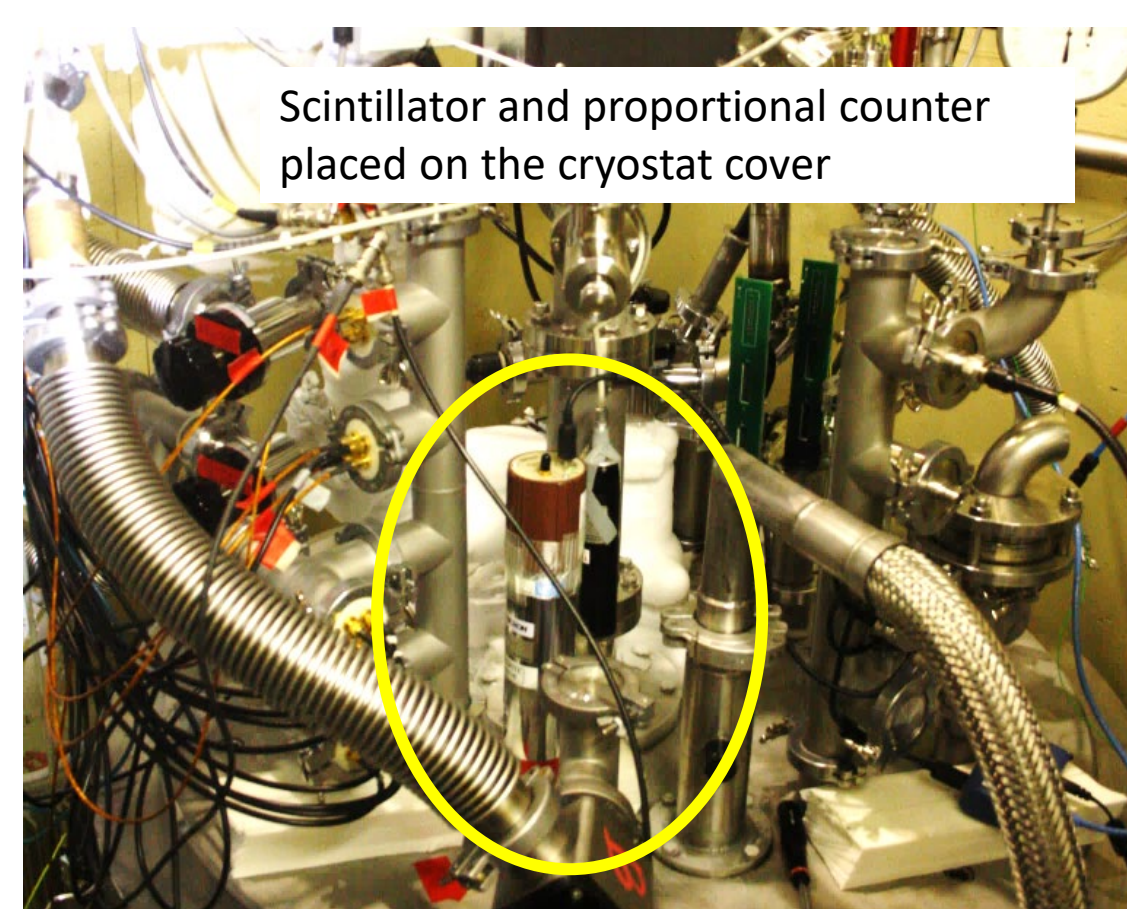
→ Ideal test bench to assess the self-consistency of the model because Q variation is only due to FE

Open points: 1) modeling the electron-to-photon count deconvolution (to exploit dose rate measurements); 2) evaluation of pile-up statistics; 3) convergence of the model when sampling with smaller φ steps to find a balance between computational speed and model accuracy

Experimental setup

To analyze **FE**, from a practical point of view:

- External radiation detectors:** portion of the impact electron energy converted to X ray Bremsstrahlung radiation.
 - Gas-filled Xe proportional counter:** to monitor the **dose rate** and partially simulate the **power** drained by **electron dark current**.
 - NaI(Tl) scintillator:** to capture the **X-ray** spectrum, enabling the evaluation of endpoint, except in case of severe pile-up events determined by poor shielding.
- Inner diagnostic devices:** electron pick-up probe and photodiodes.
- Cavity Q-drop measurement:** to evaluate the **overall power** of FE if it is the dominant factor limiting the performance.



Field-dependent effect of FE on the quality factor evaluated as:

$$\frac{1}{Q(E_{acc})} = \frac{1}{Q_0} + \frac{R}{Q} \frac{P_{FE}}{(E_{acc} l)^2}$$

Q_0 : quality factor without FE, l : accelerating gradient, R/Q : cavity geometric shunt impedance

Total dissipated power given $P_d = P_c + P_{FE}$, where P_c is the power dissipated in cavity walls.

Model of Field Emission

- Combination of experimental investigation and theoretical framework to ensure consistency between model and measurements.
- Experimental observables used to establish a self-consistent model: **dose rate**, **energy endpoint** and **Q-drop** → determination of key parameters such as **emitter position**, **emitter size** and **field enhancement factor**.
- FishPact** program (2D model for electron energies and tracking simulations) used as a starting point, to simulate **pure FE** events (multipacting events are neglected) → electron absorbed upon its first impact with the cavity walls.

Pro and cons of FishPact: lack of advanced post-processing features and emission models, but faster computational speed.

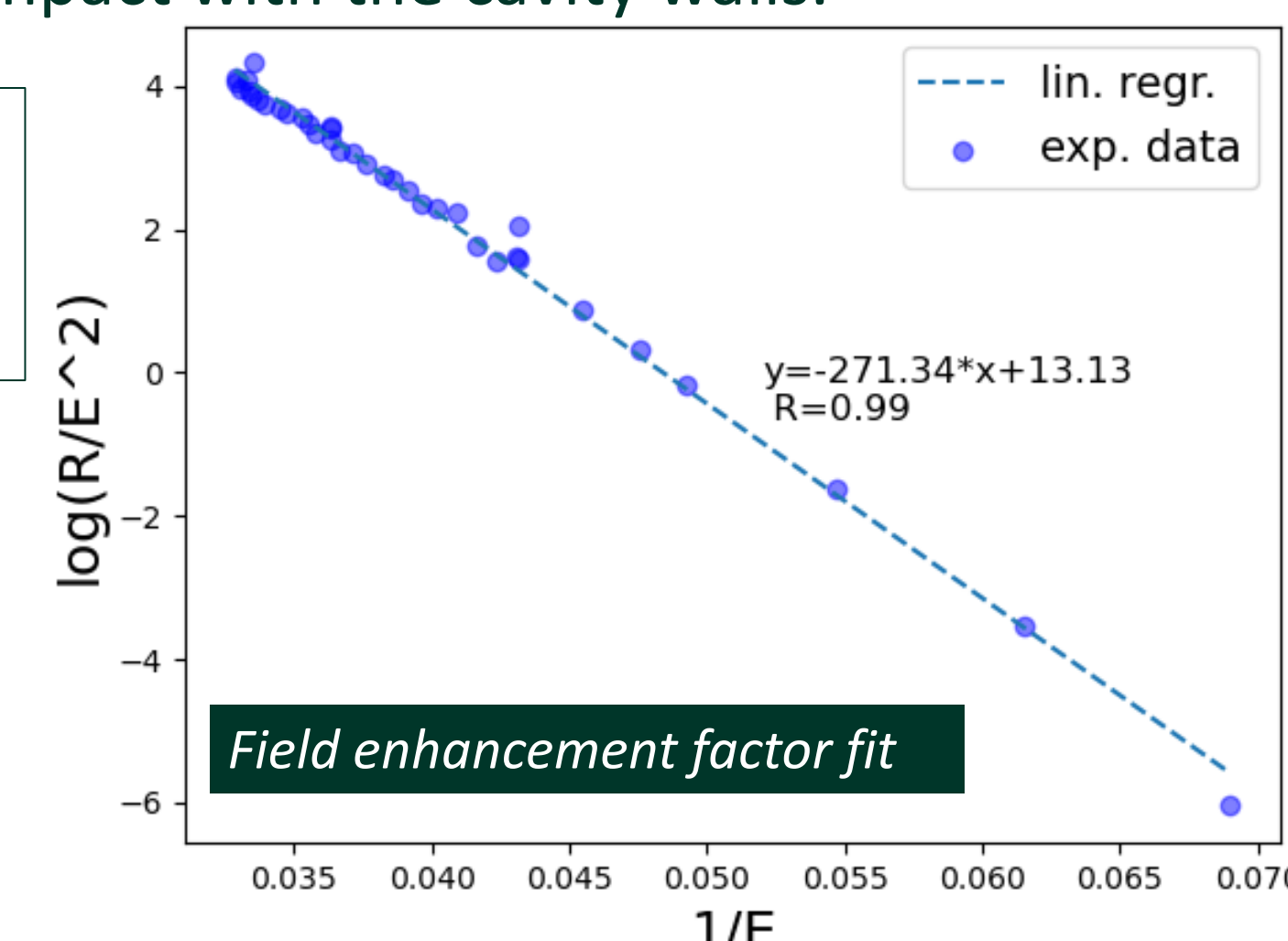
Field enhancement factor (β):

- Considers the field emitter **geometry**
- Can be computed by fitting the **FN** equation with the **dose rate**

$$\log \frac{R}{E^2} = \log A - \frac{B}{\beta E} \quad \text{A and B are coefficients}$$

Dose rate expected to be proportional to the **electron current**:

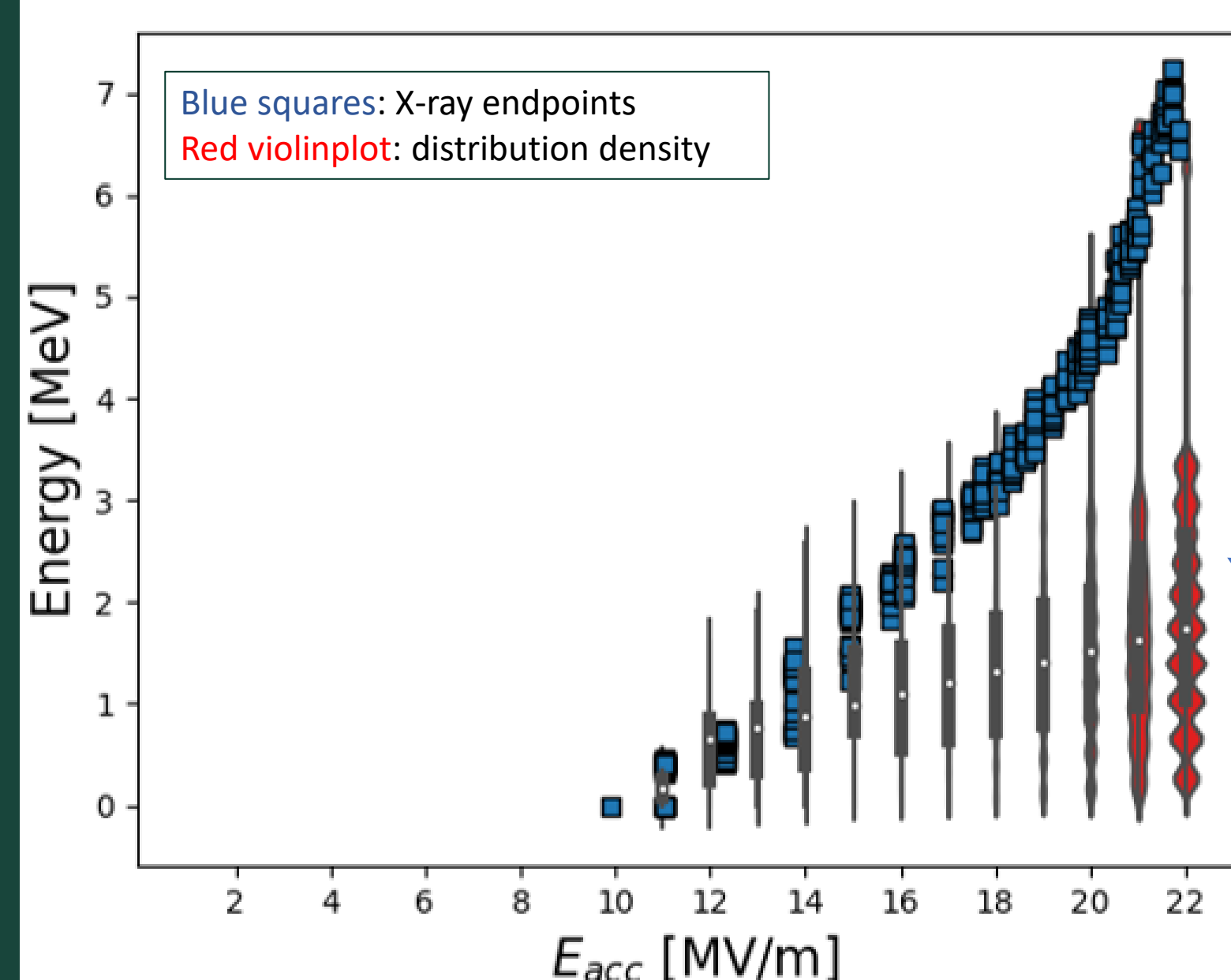
$$R \propto \frac{1}{T} \int N(E) dE$$



FN fit performed for exploiting the angular coefficient of the derived curve.

- Procedure applied to the case of **B61-EZ-002 PIP-II** prototype cavity
- Estimated value of $\beta \sim 250 - 300$.

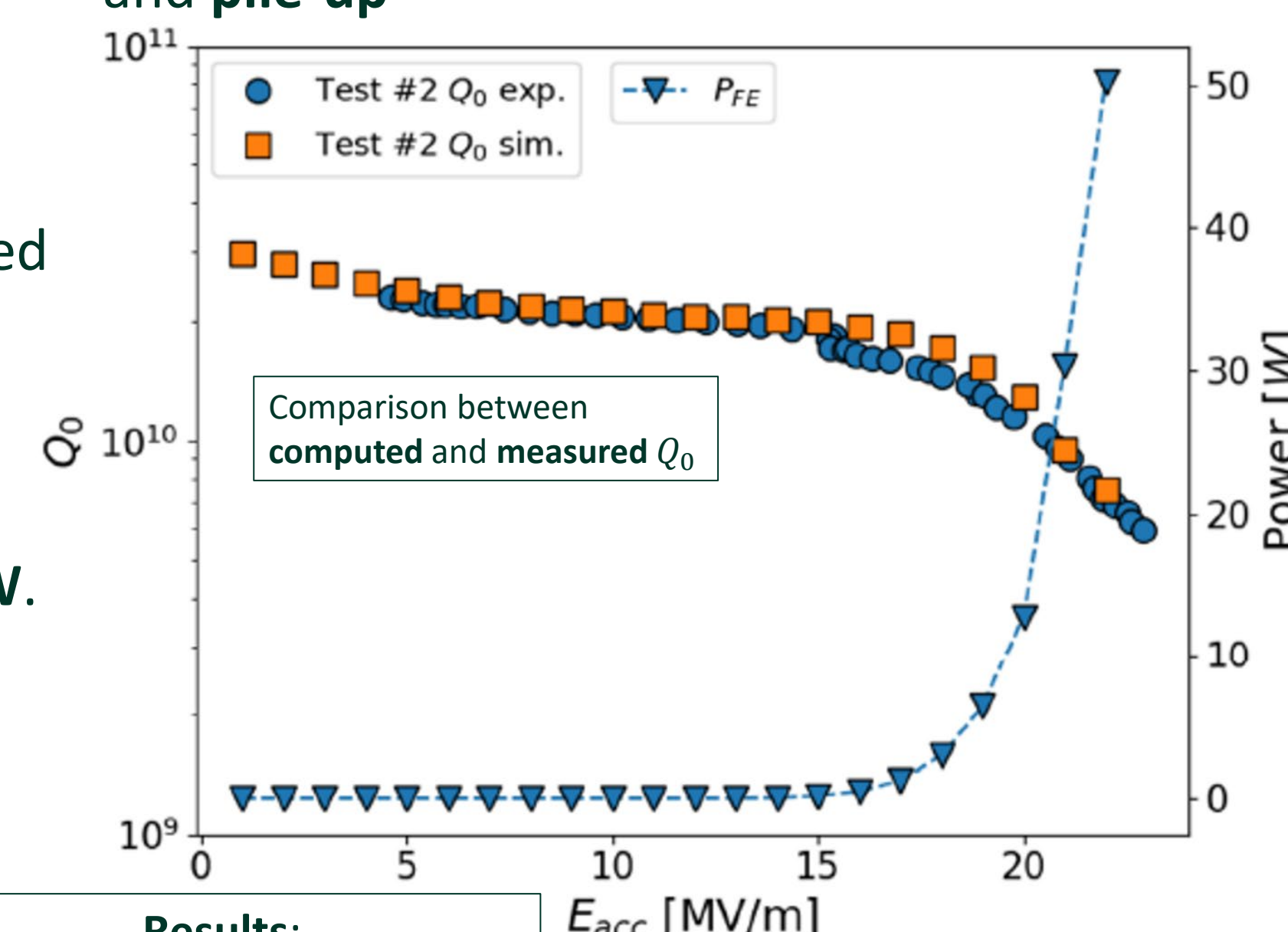
Case study simulation results



- Numerous FishPact simulations, varying E_{acc} , **emitter site position** and **size**.
- 1st step:** calculation of E_{acc}/E_{peak} for all coordinates
- Leveraging FishPact *.out* files, a script discretized **FN** law within a given range of E_{acc} and φ and applies it to electron trajectories to obtain the **probability** distribution.

Reconstructed **density distribution**, compared to **X-ray endpoints** → good agreement between computed and measured data up to 20 MV/m. At higher fields: detector **saturation** and **pile-up**

- Good **agreement** between computed and measured Q_0 → satisfactory solution for estimating position and size of the suspected emitter site.
- Computation of the **power** due to FE (plot in the right Fig.) → **power** begins to rise @ ~19 MV/m and @ 20 MV/m it reaches **12 W**.



Results:
 $\beta = 300$
emitter $A = 1.5 \times 10^{-15} m^2$
emitter position nearby iris 2